Assessment of the design, operation, and economy of the seawater reverse osmosis plant in Al-Jubail region, Saudi Arabia

Irfan Wazeer[a], Salah Ud-Din Khan[b,c],*, Ibrahim S. Al-Mutaz[a], Ibrahim M. AlAteeq[a], Achmad Chafidz[d], Shahab Ud-Din Khan[e]

[a]*Chemical Engineering Department, King Saud University, P.O. Box: 800, Riyadh 11421, Saudi Arabia,*
emails: iwazeer@ksu.edu.sa (I. Wazeer), almutaz@ksu.edu.sa (I.S. Al-Mutaz), iateeq@hotmail.com (I.M. AlAteeq)
[b]*Sustainable Energy Technologies Center, College of Engineering, King Saud University, P.O. Box: 800, Riyadh 11421,*
Saudi Arabia, email: drskhan@ksu.edu.sa
[c]*K.A. CARE Energy Research and Innovation Center in Riyadh, Riyadh, Saudi Arabia*
[d]*Department of Chemical Engineering, Universitas Islam Indonesia, Yogyakarta 55584, Indonesia, email: achmad.chafidz@uii.ac.id*
[e]*Pakistan Tokamak Plasma Research Institute (PTPRI) P.O. Box: 3329 Islamabad, Pakistan, email: shahab.furqan@gmail.com*

Received 22 June 2020; Accepted 25 January 2021

ABSTRACT

The aim of this study is to conduct performance evaluation of a seawater reverse osmosis plant located in Jubail, Arabian Gulf, via the development of theoretical and computational models. A simulation package was used to validate the simulated data against the real plant data, and resulted in good agreement with the actual plant data. A parametric analysis was also performed to study the effect of various parameters for a broad range of design considerations. Most of the previous studies involved the modeling of single-stage RO process; however, in the current work, we investigated both single- and two-stage RO systems. Besides, detailed economic assessment was also conducted in terms of standardization in design and cost analysis by utilizing a theoretical and computational model. Results indicated that with enhancing recovery ratio from 25% to 40%, maximum flux of 34.13 lmh was obtained for single-stage RO system. The economic analysis predicted that fuel ratio corresponded to power utilization factor constitute about 62% of the total cost of the plant. Another important aspect is to calculate the effect of membrane life on TDS values annually and it was concluded that the most stable values were achieved during month of April.

Keywords: Reverse osmosis; Theoretical model; Simulation; Techno-economical model; Verification and validation; Economically viable plant

1. Introduction

In the developing nations, one of the ultimate challenges is the inadequate delivery of drinking water. Water is known as one of the world's most abundant and substantial compounds; nonetheless, it is an irrefutable fact that the resources of freshwater are radically being reduced due to human consumption across the globe [1–4]. Consequently, various desalination processes have been used to produce drinking water in order to overcome the growing demand for clean water [5,6]. Presently, many countries, especially in the Persian Gulf, are employing desalination technologies to produce drinkable and industrial water for their supplies [7,8]. The reverse osmosis (RO) process became more competitive with the traditional thermal desalination technologies in the 1980s, and the worldwide installed capacity of RO systems across the globe has been surpassing the thermal technologies since the mid-1990s.

RO process depends on a property of specific polymers called semi-permeability in order to remove ions.

* Corresponding author.

Such semi-permeable membranes have high permeability for water, while low permeability for dissolved substances [9,10]. In the RO process, a particular pressure difference is applied across the membrane, which forces feed water to permeate through the semi-permeable membrane. In order to subdue the osmotic pressure of the feed side, the quite high feed pressure is essential, which usually ranges from 55 to 68 bar in seawater desalination. Due to the lower feed-water salinity of brackish water, the osmotic pressure is also low for the purification of water. Fig. 1a depicts the simplified flow process of the RO process. Desalination plants operating via the RO process primarily entail four major sections: (1) pretreatment section, (2) membrane systems, (3) high-pressure pumps, and (4) post-treatment section [5].

In an RO system, the majority of entropy generation can be related to the permeate flow via the membrane. One convenient way of reducing the entropy generation or energy consumption is by including a second stage to the conventional one-pass RO process, as shown in Fig. 1b. This is achieved by adding an intermediate pump between the RO stages. The feed is initially taken to the first-stage feed pressure in order to prevent pressurizing the whole feed to a very high pressure. In the first step, some permeate is generated, and then the brine is taken to the second-phase feed pressure. In the next stage, the remaining permeate is produced. Each stage consists of certain number of pressure vessels with RO membranes. Performance study of RO processes usually deals with the monitoring of plant productivity, quality of produced water, brine disposal, and recovery during a certain period of time.

Various studies were conducted to investigate the performance of reverse osmosis plant in the Gulf Region. Al-Bastaki and Abbas [11] developed a simplified model based on the solution diffusion membrane mass transport phenomena to predict the performance of hollow fiber RO membranes. They considered different parameters including concentration polarization (CP), bulk solution concentration variation, and the drop in pressure in the fiber
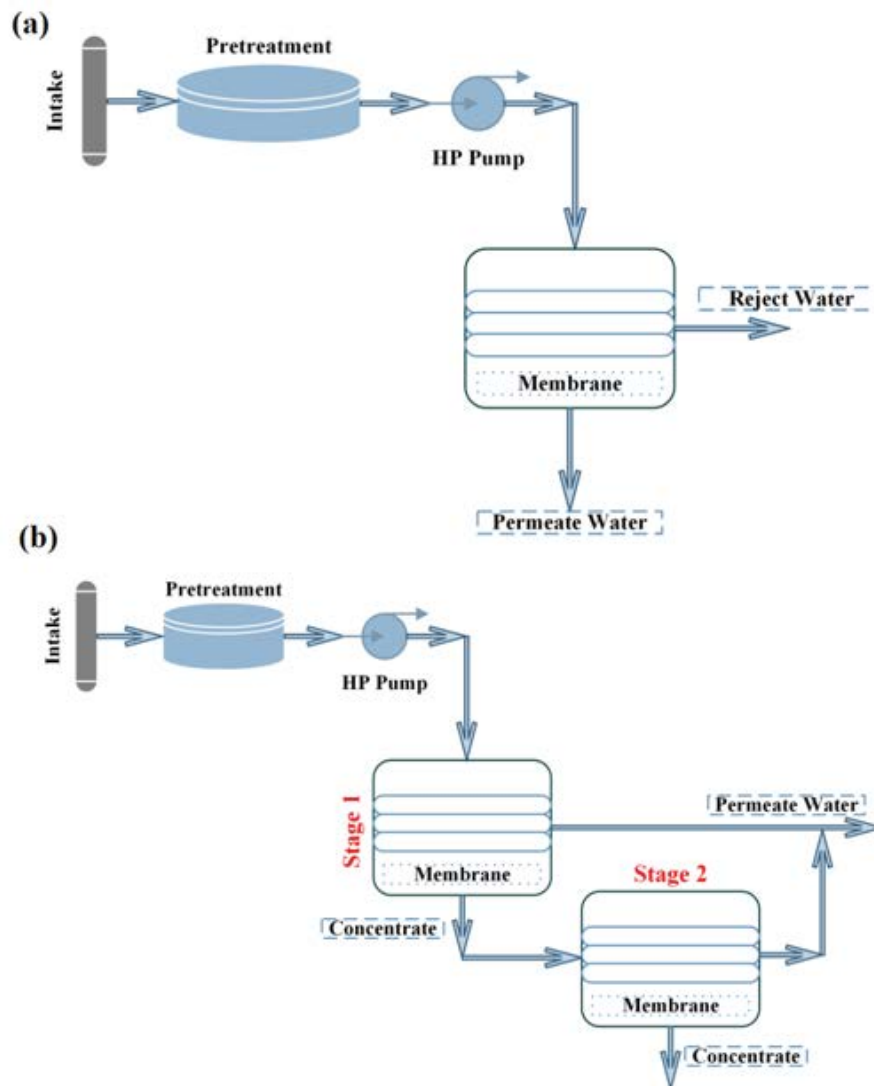

Fig. 1. Simplified flow diagram of (a) single-stage reverse osmosis (RO) process and (b) two-stage RO process.

bundle and fiber bore. They obtained good agreement between model data and the industrial RO plant data for hollow fiber RO membranes. However, a more systematic approach would yield improved results.

Kaghazchi et al. [12] developed a mathematical model to study the performance of two industrial desalination plants in the Persian Gulf region. They developed a semi-rigorous mathematical model and compared the results with the plant's operational data. For the first industrial plant and for the second industrial plant, relative errors in the water recovery and salt rejection were 10.03% and 0.03%, and 3.1% and 0.07%, respectively. The effect on the plant efficiency of performance parameters including pressure and feed flux were investigated. The increase in pressure resulted in a non-linear increase in flux due to the accumulation of salt along the membrane surface. Furthermore, an increase in the feed water flow rate reduced the permeate concentration because the mass transfer coefficient increased due to higher feed flow rate and CP factor approached unity.

Atab et al. [13] conducted a numerical analysis to study the performance of RO membrane for a desalination process. Thermolib and Matlab/Simulink were used to develop the mathematical model for a case study based in Iraq. In order to establish efficiencies and reduce losses, a thorough mathematical analysis was performed. They studied the effect of various parameters including feed pressure, feed water temperature, recovery ratio, and salinity. Moreover, economic assessment of RO system was also conducted. The study using the developed model indicated that salt discharge could be decreased from 97% to 88% in order to deliver large volumes of fresh water with agricultural acceptability (lower quality).

Al-Sahali and Al-Qattan [14] conducted a detailed analysis in terms of operating and design characteristics of a small RO plant located in Kuwait. A solution diffusion model and costing analysis were performed and results were compared against the plant performance. They obtained reasonable agreement with the plant data in regard with the salt permeability coefficient. The normalized plant data over a 1-y period was used for the evaluation purpose. During the simulation of plant characteristics through algebraic and differential forms of the solution diffusion model, permeability data were used along with other plant characteristics. Fairly uniform production rate was obtained via the adjustment of operating pressure, membrane cleaning and feed flow rate.

Al-Shayji and Liu [15] presented practical guidelines and methodology to develop predictive models for large-scale desalination plants. They used data-based and model-based approaches for developing predictive models. They used actual operating data of RO plant located in Saudi Arabia. Data-based neural networks model was able to successfully predict the performance variables of RO desalination plant. They suggested to use a data-based model when it is difficult to develop a model-based process simulation. However, the precision of a neural network model relies on the proper choice of input variables. For instance, neural networks model will not generate favorable results if the data are not within the range with which the network is trained. The neural network can precisely interpolate data, but sometimes does not extrapolate it correctly. On the other hand, different tools available in the model-based approaches (such as sensitivity analysis tool) will help to measure effectively the impact of various operating variables on desalination output variables.

A parametric analysis has been conducted by the Saline Water Conversion Corporation on three seawater reverse osmosis (SWRO) plants [16]. This study includes the 4,400 m³/d Ummlujj plant, the 2,275 m³/d Al-Birk plant, and the 12,000 m³/d Jeddah plant. A continued work was done to include the study of the performance of five more SWRO plants. This study includes Al-Birk plant, Umm Lujj plant, Jeddah-I plant, Duba plant, and Hagl plant [17]. These two studies have shown that the product quantity, product quality, and plant availability, as well as the annual decline in the total capacity, and salt rejection of these plants were varied with time. Mobayed et al. [18] investigated the features of polyamide hollow fine fiber and polyamide spiral-wound (SW) membranes in the Al-Jubail SWRO desalination plant. The objective of their study was to investigate the performance of different parameters such as feed water pressure, salt rejection, and flux decline of the two types of membranes. Al-Mutaz and Al-Sultan [19] predicted the plant performance of the RO system by utilizing the complete mixing model. The proposed model was validated against the operating data of the Manfuhah (Saudi Arabia) RO system.

The principle objective of this research is to conduct a performance evaluation of the SWRO plant in Jubail. The study includes the monitoring of product flow and quality of water during longer operational period (over a 1-y period) of the plant. We have collected the intensive plant operated data to analyze and compare with the theoretically developed model. The verification and validation concept is used to compare the plant operational data, by developing theoretical and computational models. Besides, the economic assessment of the SWRO system is also performed for the cost-effectiveness of the plant. The results obtained from the plant, as well as with theoretical calculations demonstrate the technical and economic feasibility of the Al-Jubail plant.

2. Research methodology

The work structure consists of: (1) description of the SWRO plant, including its operation and design limits, (2) theoretical and computational assessment of the SWRO plant, (3) verification and validation (V & V) analysis and (4) an economic assessment of the plant.

3. Description of the SWRO plant including the operation and limits in the design

Construction of the Al-Jubail SWRO plant started in 1994 and ended in 1998, with the commissioning period running from September 2000 to January 2001. The SWRO plant has 15 RO trains, each with a capacity of 253 m³/h. The salient features of this plant are summarized in the following sections.

The plant has been designed for an output of at least 20 MIGD under the design conditions;

- Raw seawater with 42,000–46,500 ppm TDS.
- Raw seawater at temperatures between 20°C and 35°C

As well as the general requirements described in International Standards for drinking water such as the WHO guidelines, the following has been guaranteed:

- TDS < 450 mg/L
- Chlorides < 250 mg/L

The input feed data are presented in Table 1. The module and stages used have also been selected in this section.

The plant has been designed to produce 20 MIGD of potable water using RO technology and operates using single-pass RO with a recovery ratio of 35%. RO membranes need to be protected from fouling in order to ensure reliable operation; a complex pretreatment system was, therefore, designed to produce optimum quality in the RO feed water. Post-treatment of the RO permeate renders the produced water potable. The layout of the SWRO Al-Jubail plant is presented in Fig. 2.

The plant was constructed using a modular design so that sections of the plant can be operated or shut down for maintenance without interrupting the operation of other sections.

4. Theoretical and computational assessment of the SWRO system

4.1. Theoretical modeling

The operating conditions and the quality of the feed water both affect the performance of SWRO plants significantly. Precise membrane transport equations for a steady-state system with distributed parameters can be attained using film theory and the solution-diffusion model [20]. The mass balance equations for the RO membrane in terms of fluid and solute are as follows:

$$Q_p = Q_f - Q_r \tag{1}$$

Table 1
Operating conditions/parameters in the Al-Jubail seawater reverse osmosis plant

Parameter	Value
Feed pH	6.5
Temperature	35°C
Permeate flow	6,072 m³/d
Permeate pressure	1 bar
Membrane life	7 y
Membrane replacements	12%/y
Max. pressure for HJ9155 module	84 bar
Feed pressure	82 bar
Brine pressure	80 bar
Pump efficiency	83%
ERT efficiency	81.85%
RAW water pH	8.2
Number of trains	15

$$Q_f C_f = Q_r C_r + Q_p C_p \tag{2}$$

$$Q_p = n_l w \int_0^L J_v \, \mathrm{d}z \tag{3}$$

where subscripts p, f, and r denote the permeate, feed, and reject (brine), respectively. C and Q represent salt concentration and flow rate, respectively.

Permeate flux is the amount of permeate obtained during the membrane separation per unit of time and RO membrane area (S_a):

$$J_v = \frac{Q_p}{S_a} \tag{4}$$

Salt rejection (R) is a proportion the solute that is retained by the RO membrane:

$$R = \left(1 - \frac{C_p}{C_f + C_r}\right)100 \tag{5}$$

The Kimura-Sourirajan model [21–25], which is related to the mass transfer coefficient, can be used to calculate the salt and local water flux. L and W refer to the length and width of the RO module, respectively, while n_l represents the number of leaves.

It was assumed that the solution–diffusion model is valid for the transport of solute and solvent through the membrane. According to the solution-diffusion model, the following equations were used to express the solute flux J_s and solvent flux J_v through the membrane [26–28]:

$$J_v = A_w \left(P_f - P_d - P_p - \Delta\pi\right) \tag{6}$$

$$J_S = B_S \left(C_m - C_b\right) \tag{7}$$

Assuming that:

$$P_b = P_F - P_d \tag{8}$$

$$\Delta P = P_b - P_p \tag{9}$$

then:

$$J_v = A_w \left(\Delta P - \Delta\pi\right) \tag{10}$$

Specific flux = flux/applied pressure
Specific flux can be described as a comparison of the performance of one kind of membrane with another as not all membranes are examined at the same pressure.

A_w is the solvent transport parameter, P_f is the feed pressure, P_d is the pressure drop along an RO SW module, P_b is the pressure along the channel of the SW module, and P_p is the pressure at the permeate side, which in general is assumed to be the same as the environmental pressure. $\Delta\pi$ refers to the loss of osmotic pressure. B_s denotes the solute transport parameter, C_m and C_{sp} are the concentration of the solute at the membrane surface on the feed side and
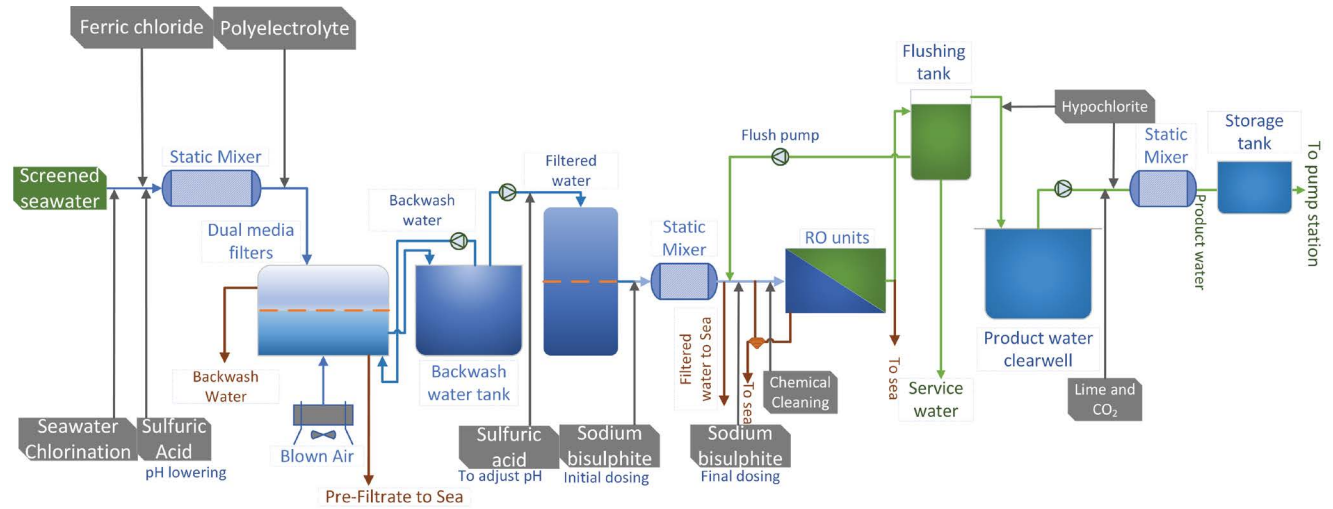
Fig. 2. Layout of the seawater reverse osmosis Al-Jubail plant.

the permeate side, respectively, and C_p is the value of C_b at the end of the module. This means $C_p = C_b(L)$. A_w and B_s are relatively sensitive to operating temperature; this relationship is represented as follows [20,26,28] by the following:

$$A_w = A_{w0} \exp\left(\alpha_1 \frac{T-273}{273} - \alpha_2\left(P_f - P_d\right) \right) \tag{11}$$

$$B_s = B_{s0} \exp\left(\beta_1 \frac{T-273}{273} \right) \tag{12}$$

where A_{w0} and B_{s0} are defined as the intrinsic transport parameters in standard condition while α_1, α_2, and β_1 are the constant parameters for transport. The operational temperature is expressed by T. Following as the following expression demonstrates an almost linear relationship between osmotic pressure and concentration [29]:

$$\Delta\pi = RT\left(C_m - C_p\right) \tag{13}$$

Here R denotes the gas law constant.

Knowledge of the different RO parameters, process specifications, and solute concentration at the membrane boundary (which is relatively different from the bulk concentration because of CP) is required in order to solve the above system of equations. The following simple relationship is, therefore, developed based on the steady-state across the boundary and CP theory:

$$\phi = \frac{C_m - C_p}{C_b - C_p} = \exp\left(\frac{J_V}{K_c} \right) \tag{14}$$

Both C_b and J_V vary across the membrane channel. The mass transfer coefficient K_c is computed by using the following relation [30]:

$$Sh = \frac{K_c d_e}{D_{AB}} = 0.065\,Re^{0.875}\,Sc^{0.25} \tag{15}$$

where

$$Re = \frac{\rho V d_e}{\mu} \tag{16}$$

$$Sc = \frac{\mu}{\rho D_{AB}} \tag{17}$$

ρ is the density of permeate water, d_e is hydraulic diameter of the feed spacer channel, μ is kinematic viscosity, and D_{AB} is dynamic viscosity; it can be obtained from the regression equation [31–33]:

$$D_{AB} = 6.725 \times 10^{-6} \exp\left(0.1546 \times 10^{-3} C_b - \frac{2,513}{273.15+T} \right) \tag{18}$$

The relationship between J_V and J_s is [34]:

$$J_S = J_v C_p \tag{19}$$

The pressure loss along the RO module can be formulated as [20,30] follows:

$$\frac{dP_d}{dz} = -\lambda \frac{\rho}{d_e} \frac{V^2}{2} \tag{20}$$

where

$$\lambda = 6.23 K_\lambda\, Re^{-0.3} \tag{21}$$

K_λ is known as the empirical parameter. As the pressure across RO channel is: $P_b = P_f - P_d$.

$$\frac{dP_b}{dz} = -\frac{dP_d}{dz} = \lambda \frac{\rho}{d_e} \frac{V^2}{2} \tag{22}$$

At $z = 0$, $P_b = P_f$, at $z = L$, $P_b = P_r$.
where V is the axial velocity on the feed side, satisfying:

$$\frac{dV}{dz} = -\frac{2J_v}{h_{sp}} \tag{23}$$

At $z = 0$ $\quad V = V_f = \frac{Q_f}{n_e W h_{sp}}$ \hfill (24)

At $z = L$ $\quad V = V_r = \frac{Q_r}{n_e W h_{sp}}$ \hfill (25)

h_{sp} denotes the height of the feed spacer channel.

The bulk concentration C_b changes across the membrane and can be given as [35] follows:

$$\frac{dC_b}{dz} = \frac{2J_v}{h_{sp}V}(C_b - C_p) \tag{26}$$

At $z = 0$, $C_b = C_f$; at $z = L$, $C_b = C_r$

After solving these equations, both Q_p and C_p can be calculated at specific operating conditions and membrane specifications, from which the recovery rate (Rec) of water and the specific energy consumption (SEC) can be obtained using the following equations [13]:

$$\text{Rec} = \frac{Q_p}{Q_f} \tag{27}$$

$$\text{SEC} = \frac{P_f Q_f / \varepsilon_p - P_r Q_r \varepsilon_{ef}}{Q_p} \tag{28}$$

where ε_p refers to the mechanical energy and ε_{ef} refers to the energy recovery efficiency.

Salt passage (Sp) and rejection coefficient (Ry) are two significant factors that reflect the performance of the RO system [36]:

$$\text{Sp} = \frac{C_p}{C_f} \times 100\% \tag{29}$$

$$\text{Ry} = \frac{C_f - C_p}{C_f} \times 100\% \tag{30}$$

Recovery (called "conversion") is used to outline what percentage volume of the influent water is "recovered" from the permeate stream. In general, the recovery that results from the SWRO process ranges from 30% to 60% [37,38]. Some two-stage RO plants with higher recovery ratio are listed in Table 2.

The percentage recovery is obtained by using the following correlation:

$$\%\text{Recovery} = \left(\frac{\text{permeate flow}}{\text{feed flow}}\right) \times 100 \tag{31}$$

The chemical characteristics of the SWRO Jubail plant seawater are summarized in Table 3.

4.2. HOLLOSEP computation

"HOLLOSEP" is a membrane module that enables high purity permeate water to be generated via ion rejection. The membrane can be used to produce quality drinking water from seawater and de-mineralize quality water from urban and industrial water for the production of medicine. In industry, HB and HJ series of HOLLOSEP membrane were employed for the replacement of the Dupont model B-10 series membranes. HB series (HB10255 and HB10255FI) models consist of two elements. The two symmetrical elements located in the pressure vessel are comprised of hundreds of thousands of hollow fibers that are circumferentially over-layered at an angle and fixed in place with epoxy resin. The controlled uniform tension and epoxy resin provides mechanical stability to the membrane element. HJ series (HJ9155) consists of one membrane element; the overall construction and flow patterns of a "HOLLOSEP" single element module are depicted in Fig. 3. The hollow fibers at both ends of the element are precisely cut in order to allow product water to be discharged from the hollow fiber pores.

The circumferential over-layered fiber configuration in which fibers cross each other is superior to simply aligned parallel fibers. The advantage lies in the significant amount of space between fibers minimizing the drop in internal pressure. This, in turn, optimizes the hydraulic design and

Table 2
Two-stage RO plants with higher recovery rate

Plant	Country	Capacity (m³/d)	Recovery rate (%)	Ref.
Kindasa	KSA	26,800	50	[40]
Valdelentisco		140,000	50	[38]
Rambla Morales		60,000	58	[41]
Maspalomas II		26,200	60	[42]
Las Palmas III	Spain	86,000	50	[43]
Fukuoka	Japan	50,000	60	[44]
Curacao	Netherlands Antilles	10,200	58	[42]

Data are taken from the study by Kim et al. [39].

Table 3
Chemical characteristics of feed seawater

Elements	Average composition		Worst case	
	mg/L	ppm CaCO$_3$	mg/L	ppm CaCO$_3$
Chloride	24,090.00	33,929.58	25,600.00	36,056.34
Sulphate	3,384.00	3,522.80	3,570.00	3,716.43
Nitrate	85.19	68.69	00.00	00.00
Bicarbonate	175.68	144.00	189.00	154.92
Bromide	83.00	103.87	90.00	112.63
Fluoride	1.00	5.26	1.00	5.26
Calcium	508.00	1,266.83	540.00	1,346.63
Magnesium	1,618.00	6,652.96	1,715.00	7,051.81
Potassium	483.00	617.65	515.00	658.57
Sodium	13,440.02	29,217.43	14,239.10	30,968.02
Barium		Not stated		
Strontium	17.00	19.40	18.00	20.54
Silica	0.01	0.01	0.01	0.01
Free carbon dioxide	0.93	1.05	0.62	0.71
Total dissolved solids	43,884.90	37,774.28	46,477.11	40,045.58
pH value		8.1		8.3
Langelier index		1.3		1.5
Stiff Davis Index		0.2		0.5
CaSO$_4$ saturation	%	29.5		31.7
Temperature	°C	26.5		20.0
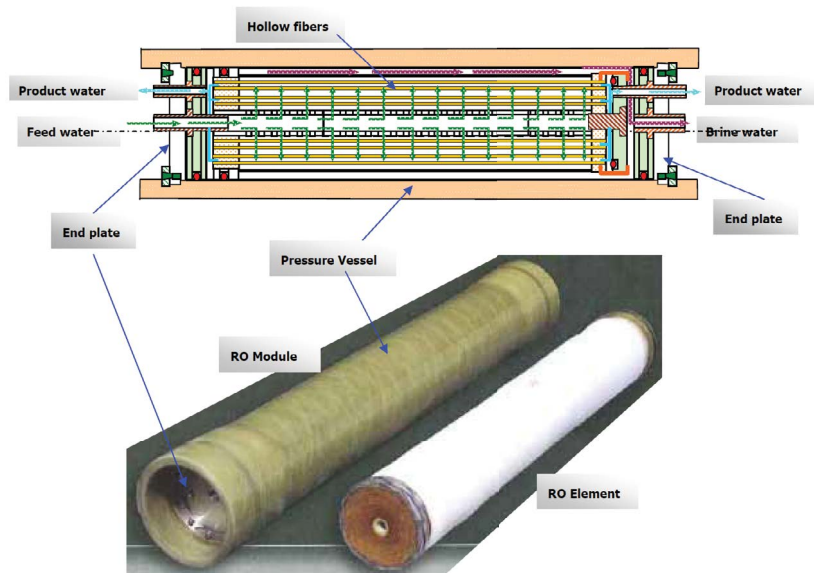
Fig. 3. TOYOBO single element type RO module (HJ9155).

prevents fouling. The HOLLOSEP HJ9155 membrane is used in the Al-Jubail SWRO plant. The specifications of the membrane are listed in Table 4.

The software used to simulate the performance of this membrane allows the designer to test many model variants without having to enter the bulk of the information repeatedly. The influent water quality is entered on the water analysis screen and users can also investigate the effects of different temperatures and the lifetime of the membrane. The section following the "calculation results" refers to energy and chemistry. In this section, feed pressure, brine pressure, permeate flow, recovery ratio, and

Table 4
Specifications of "HOLLOSEP" element model: HJ9155PI

Parameters	Value
Material used to construct membrane	Cellulose triacetate
Number of elements	1
Size, diameter	294 mm
Length	2,051 mm
Weight when filled with water	Approx. 180 kg
Connections	
Feed	NPT 1″
Product	NPT 1/2″
Brine	NPT 1″
Initial performance under Toyobo standard condition	
Product flow rate	34 (30) m³/d
Salt rejection (test conditions)	99.6 (99.4)%
Feed water (NaCl solution)	35,000 mg/L
Pressure	55 kg/cm²G
Temperature	25°C
Recovery ratio	30%
Initial performance under Dupont's condition	
Product flow rate	56 (50) m³/d
Salt rejection (test conditions)	99.8 (99.6)%
Feed water (NaCl solution)	35,000 mg/L
Pressure	1,000 psig
Temperature	25°C
Recovery ratio	35%
Operating conditions	
Pressure (max)	84 kg/cm²G
Temperature (min, max)	5°C, 40°C
Brine flow rate (min, max) *,a3	50, 150 m³/d
Feed water qualities	
FI (SDI 15)	4.0 or less
pH (min, max)	3, 6.6
Max. residual chlorine	0.5 mg/L

aThe brine flow rate range is limited by the temperature and quality of the feed water.

pump efficiency entered as input parameters that will result in pumping energy, recovered energy, and the amount of energy required for the process. The plant flow section provides an overview report of the process, providing an overview of the configuration of the system and the flow rates for each channel.

5. Verification and validation (V & V) analysis:

5.1. Validation of the theoretical model with HOLLOSEP

Eq. (24) can be applied to calculate the absolute deviation of the simulation program from the plant data [45]:

$$\text{Deviation} = \frac{\left| i_{\text{act}} - i_{\text{sim}} \right|}{\left| i_{\text{act}} \right|} \times 100\% \tag{32}$$

where i_{act} is the actual plant data and i_{sim} is the simulated value.

The permeate parameters from the simulated HOLLOSEP and the actual plant are compared in Table 5, in which the absolute deviation of each permeate parameter is given. Overall, it was noted that the quality of the simulated permeate was in good agreement with the plant data in terms of pH, hardness, and TDS ions. However, high deviation was observed for some individual ions; this could be due to the fact that the software was not fed with the concentration of some chemicals, which often used in the actual plant. Normally, ions behaved somehow different than the theoretical prediction. Nonetheless, the deviations between the actual plant data and HOLLOSEP simulation results for pH, hardness, and TDS are small at 0.0%, 9.09%, and 4.47%, respectively. This indicates that the HOLLOSEP membrane worked efficiently in extracting the TDS from seawater; the permeate content (permeate quality) is in compliance with the Drinking Water Quality Standards (DWQS). The plant flow using HOLLOSEP is presented in Fig. 4.

6. Results and discussion

In this section, some of the key terms are described and an explanation of the factors that affect the quality of RO membranes, such as temperature, pressure, feedwater flow rate, permeate recovery, the number of membrane elements, and pH of water is given.

Feed flow is the rate at which feedwater is injected into the membrane. Fig. 5 illustrates the impact of membrane elements used and feed flow on the TDS and flux in both one and two-stage systems. In the one stage system, the maximum flux observed was 41.31 lmh at a feed flow of 1,000 m³/h. The flux is divided into two stages (stage 1 and stage 2). For two-stage RO system, Fig. 5 shows the flux after the final stage only (second stage). The highest flux of second stage is of 20.66 lmh at the same feed flow (1,000 m³/h) in the two-stage system, using one membrane element, while average flux of two-stage RO design is same as of single-stage system (41.31 lmh at feed flow 1,000 m³/h). As seen in the figure, the number of elements influences the flux significantly in both designs. Both flux and NaCl rejection are observed to increase as the feed flow increases. At higher feed flow rates, the increase in flux is possibly attributed to an increase in the cross-flow velocity shear force at the membrane surface, which helps in minimizing the effect of external CP. The increase in cross-flow velocity shear force enhances the mass transfer coefficient of the feed and eventually leads to higher water flux through the membrane.

Fig. 5 also depicts the effect of feed flow on total TDS in both one- and two-stage designs. It is apparent that the amount of TDS within the permeate in both designs decreases when the feed flow rate is increased. The highest TDS value of 2,059.94 mg/L was achieved using four membrane elements at a feed flow rate of 400 m³/h. The minimum TDS using the single-stage system is 152.67, and 245.47 mg/L with the double stage design. Single- and two-stage RO systems depict the same pattern in terms of relationship between the operating parameters, however, two-stage system produces more permeate water and

Table 5
Comparison of the permeation parameters in the HOLLOSEP program results with actual plant data

Permeate parameters/ions	HOLLOSEP results	Actual plant data	Absolute deviation (%)
Calcium	1.4	1.3	7.69
Magnesium	4.4	4.0	10.00
Sodium	62.4	58.4	6.85
Potassium	3.0	2.9	3.45
Strontium	0.0	0.0	0.00
Bicarbonate	2.0	1.3	53.85
Free carbon dioxide	0.0	0.0	0.00
Sulphate	6.1	5.7	7.02
Chloride	108.0	101.7	6.19
Fluoride	0.0	0.0	0.00
pH	4.8	4.8	0.00
Hardness as $CaCO_3$	21.6	19.8	9.09
TDS ions	198.7	190.2	4.47
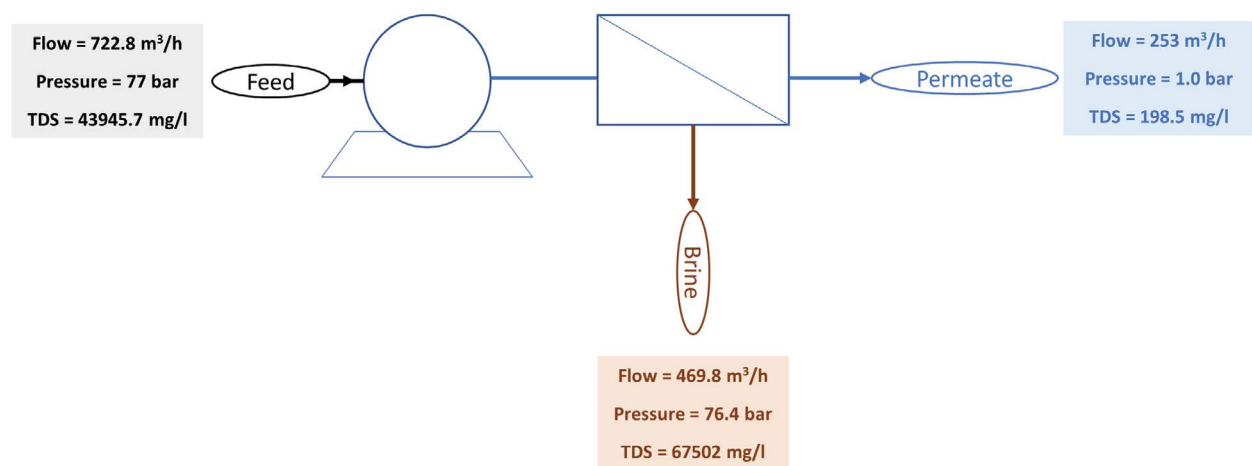
Fig. 4. Plant flow diagram using HOLLPSEP.

two-stage RO system generates higher TDS of pure water because of the higher TDS transports through the second stage.

Fig. 6 displays the effect of feed flow rate on the specific energy in both designs (single- and two-stage). As can be seen from the graph, the specific energy increases as the feedwater flow rate increases in both designs. The similar behavior was reported by Mahmoudi and Akbarzadeh [46] and Schäfer et al. [47], that is, the SEC increased with increasing feed flow rate and increasing pressure. The SEC is very high at high feed flow because of low recovery. The specific energy in the two-stage design is lower than that of the single-stage design because of the increase in the production of freshwater. Moreover, the number of membrane elements also affects the specific energy; the specific energy is reduced significantly as the number of elements is increased.

The rate of the permeation of water across the membrane increases with the temperature of the feedwater because the viscosity of the solution is decreased, allowing the water to diffuse more rapidly through the membrane [48,49]. Increasing the temperature of the feed water will, therefore, lead to lower salt rejection because of the enhanced rate of the diffusion of salt across the membrane. As shown in Fig. 7, the TDS increases gradually with temperature up to 30°C, after which a sharp rise occurs. The total TDS increases from 198.7 to 685.2 mg/L as the temperature of the feeding water is increased from 30°C to 40°C, which is a significant increase.

On the other side of the membrane, the variability in the feed pressure is reduced from 84 to 66.4 kg/cm² as the feedwater temperature rises from 10°C to 40°C, as shown in Fig. 8. The feed pressure changes slowly as the feed temperature is increased. The feed water is driven through the semi-permeable membrane via the application of pressure, as a result of which the water permeates through the pores of the membrane to be released as purified water. In generating a constant flow of product, an increase in the temperature of the feedwater means that the required feed pressure will be reduced and the salinity of the product
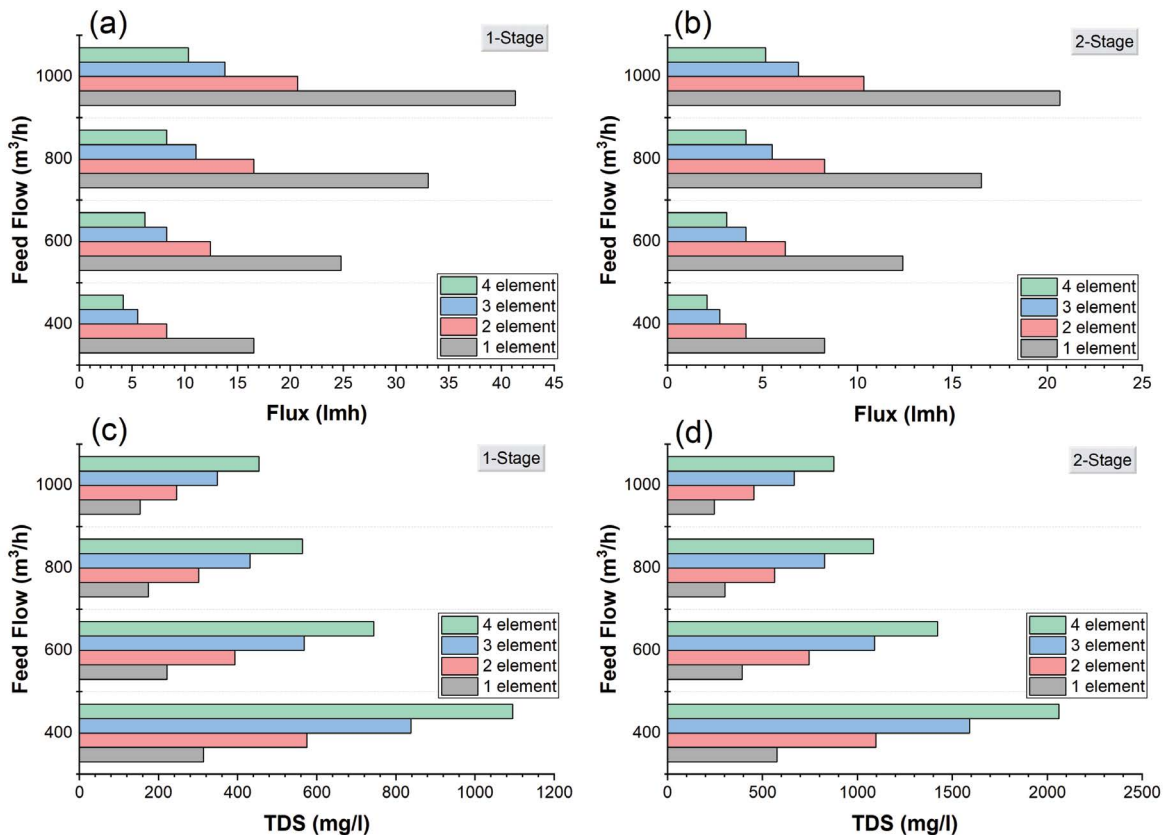
Fig. 5. Effects of the number of membrane elements and feed flow rate on (a) flux for 1-stage, (b) flux for 2-stage, (c) TDS for 1-stage and (d) TDS for 2-stage.
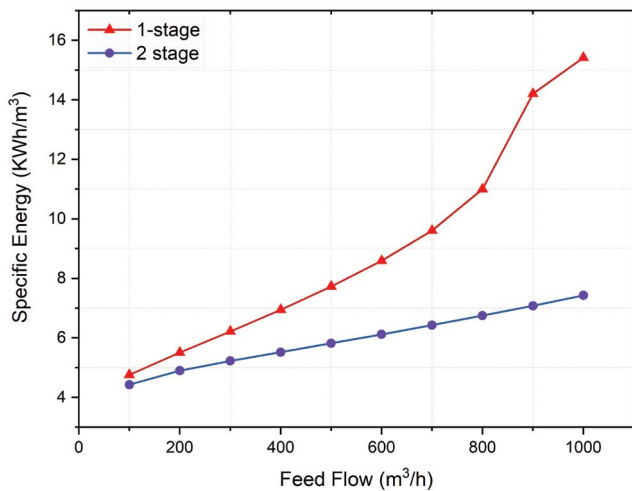

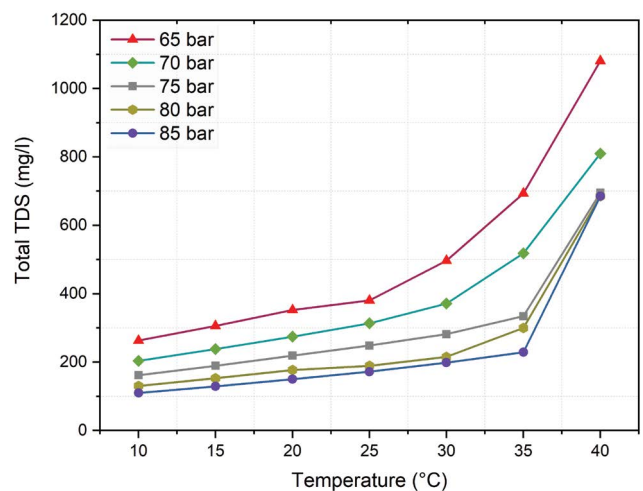Fig. 6. Effect of changes in the feed flow rate on specific energy.

Fig. 7. Effect of feed water temperature on TDS.

will increase. The energy consumption is also reduced as the feed pressure is decreased. If the flow of permeate increases with the increase in temperature, fewer membrane elements are needed, leading to substantial savings in the cost of the process.

Fig. 9 shows the relationship between the temperature of the feed water and the specific energy in both single and twin-stage RO systems. As expected, the specific energy is reduced as the temperature is increased in both designs (1-stage and 2-stage) and the required feed pressure is reduced at higher feed temperatures. It is also apparent that a two-stage design has a lower specific energy consumption than a single-stage RO system because of the higher production of permeate water. The highest specific energy of
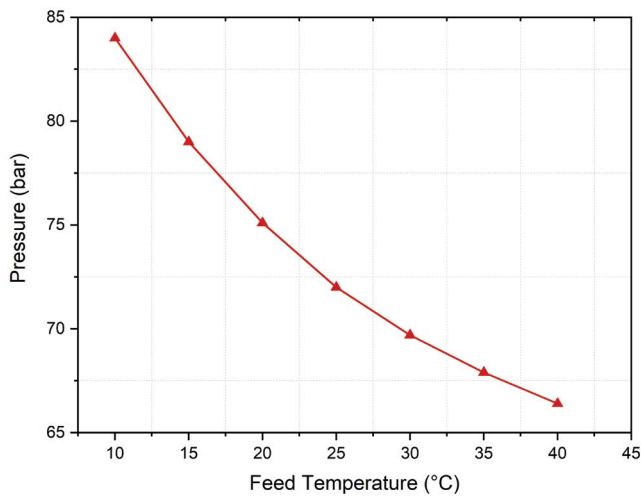
Fig. 8. Effect of feed temperature on feed pressure.

Fig. 10. Effect of feedwater pressure on salt rejection and flux.

Fig. 9. Variation in the specific energy required with feed temperature in single and double stage RO systems

13.95 kWh/m^3 was observed in a single-stage system with the lowest temperature of 10°C.

The pressure of the feed water influences both the flux of the water and the salt rejection from the RO membranes. Osmosis is the flow of water from a dilute solution to a concentrated solution via a membrane. RO involves the use of pressure to overcome the natural osmotic pressure in the feedwater stream. This extra pressure is introduced to the concentrated solution, reversing the flow of the water. Some of the feed water (on the side containing the concentrated solution), therefore, emerges as purified water from the dilute side of the membrane. Fig. 10 demonstrates how the flow of water across the membrane directly increases as the feed water pressure rises. The water supply pressure also leads to an increase in the salt rejection. As RO membranes only act as weak barriers to the salts that are dissolved in the feedwater, salt is often also propelled through the membrane.
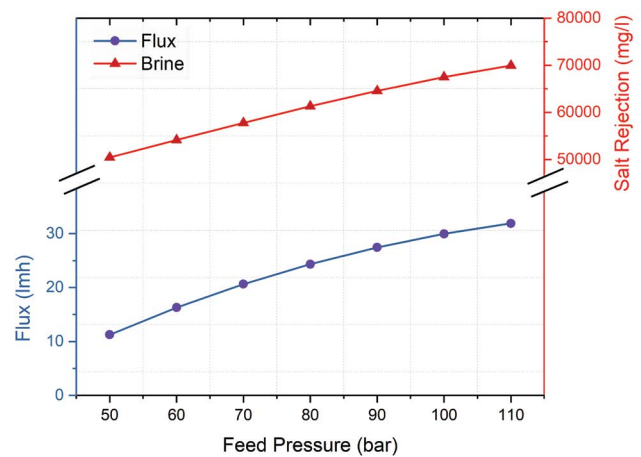
The pH influences the efficiency of the separation due to its effects on both the solute hydration and the adsorption capacity of the membrane. The pH effect of the feed water is demonstrated in Fig. 11. The pH value of the permeate increased from 1 to 8.6 with a change in the feed pH value from 3 to 8 at 30°C, as illustrated in Fig. 11a. The effect of feed pH on permeate pH is shown at different temperatures ranging from 20°C to 35°C. It is apparent that the highest values of permeate pH were attained at the higher temperature of 35°C. The maximum pH of 8.7 was achieved at 35°C with a feed pH of 8. The trend in the change of permeate pH is the same at all temperatures.

Moreover, the permeate salinity TDS changes from 90.5 to 872.9 mg/L TDS when the pH changes from 3 to 7, as illustrated in Fig. 11b. There is not much change in the TDS at lower values of pH; however, the change in the TDS is very significant at higher values of pH. For instance, the TDS increases from 198.7 to 37,323.39 mg/L when the pH is increased from 6.5 to 8.

The influence of feed pH on the specific energy was also investigated in this study. Fig. 11c shows the effect of feed pH on specific energy consumption. As can be seen, there is no significant effect from the feed pH on the specific energy except at lower values of pH. For example, when the pH is increased from 3 to 4.5, the specific energy is reduced from 9.97 to 9.88, while no change is observed in the specific energy when the pH is increased from 4.5 to 8.

Another critical parameter that affects the performance of the SWRO system is the recovery ratio. The total recovery achievable in any RO process typically relies not on the minimal osmotic pressure, but on the concentration and the tendency of salts in the feed water to precipitate onto the membrane as mineral scale. Calcium carbonate, calcium sulfate, and silica are the most common sparingly soluble salts. Chemical feedwater treatment can be applied in order to prevent mineral scaling. Fig. 12 illustrates the effect of recovery on the flux, permeate pH, flow rate, salt rejection, and TDS. The effect of recovery on flux and pH was studied for both the 1-stage and 2-stage RO systems.

It is apparent from Fig. 12 that the flux increases with the recovery ratio in both the 1-stage and 2-stage designs.
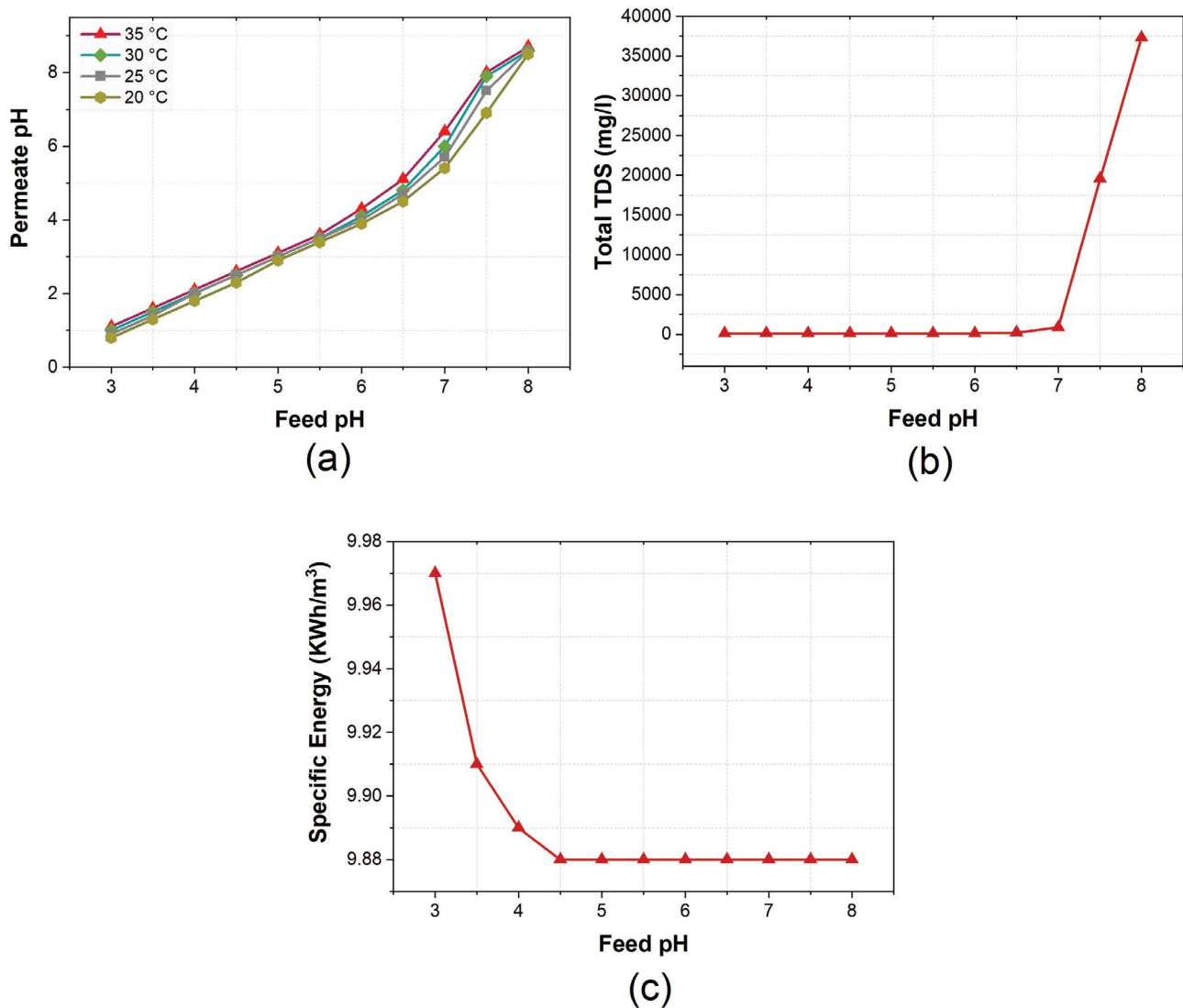
Fig. 11. Effect of feed pH on (a) permeate pH, (b) total TDS, and (c) specific energy.

The maximum flux of 34.13 lmh was achieved at the highest recovery ratio (40%) in the single-stage system. The flux is lower in the two-stage system than it is in the 1-stage system because of the higher production of freshwater. It can be concluded that a reduction in the pH results in an increase in the recovery ratio in both the single and the twin RO system. At a higher recovery ratio, there is an upsurge in the specific energy consumption, which may due to the sharp increase in the feed pressure required for higher recovery. The pH changes linearly with the change in the recovery ratio, as seen in Fig. 12.

The recovery ratio also significantly affects the flow rate of both the permeate and the brine. As suggested by Eq. (17), the recovery ratio is directly related to the flow of the permeate. The increase in the recovery ratio, therefore, leads to an increase in the permeate flow and a reduction in the brine flow. Furthermore, the increase in the recovery ratio results in an increase in the flux and the permeate flow, leading to a reduction in the permeate TDS while the increase in the

recovery ratio leads to an increase in the salt rejection. The decrease in permeate TDS with the increase in recovery ratio is due to the increase in permeate flow at higher recovery. Also, high recovery is often associated with an increase in the trans-membrane pressure, which enhances the salt passage through the membrane. An increase in the recovery ratio from 25% to 40%, reduces the TDS from 225.37 to 181.06 mg/L.

Fig. 13 depicts the effect of membrane life on TDS. Depending on the application, the average membrane life of an RO membrane element varies from 3 to 7 y, and may only last 1 to 2 y in some RO systems. The lifetime of an RO element is reliant on various factors, including the selection of the element, system design, pretreatment, membrane cleaning, system operation, and system maintenance. The RO membrane is a thin film that includes numerous microscopic pores and is considered to be one of the most critical parts in an RO system. During typical operation, the membrane can become contaminated by biological
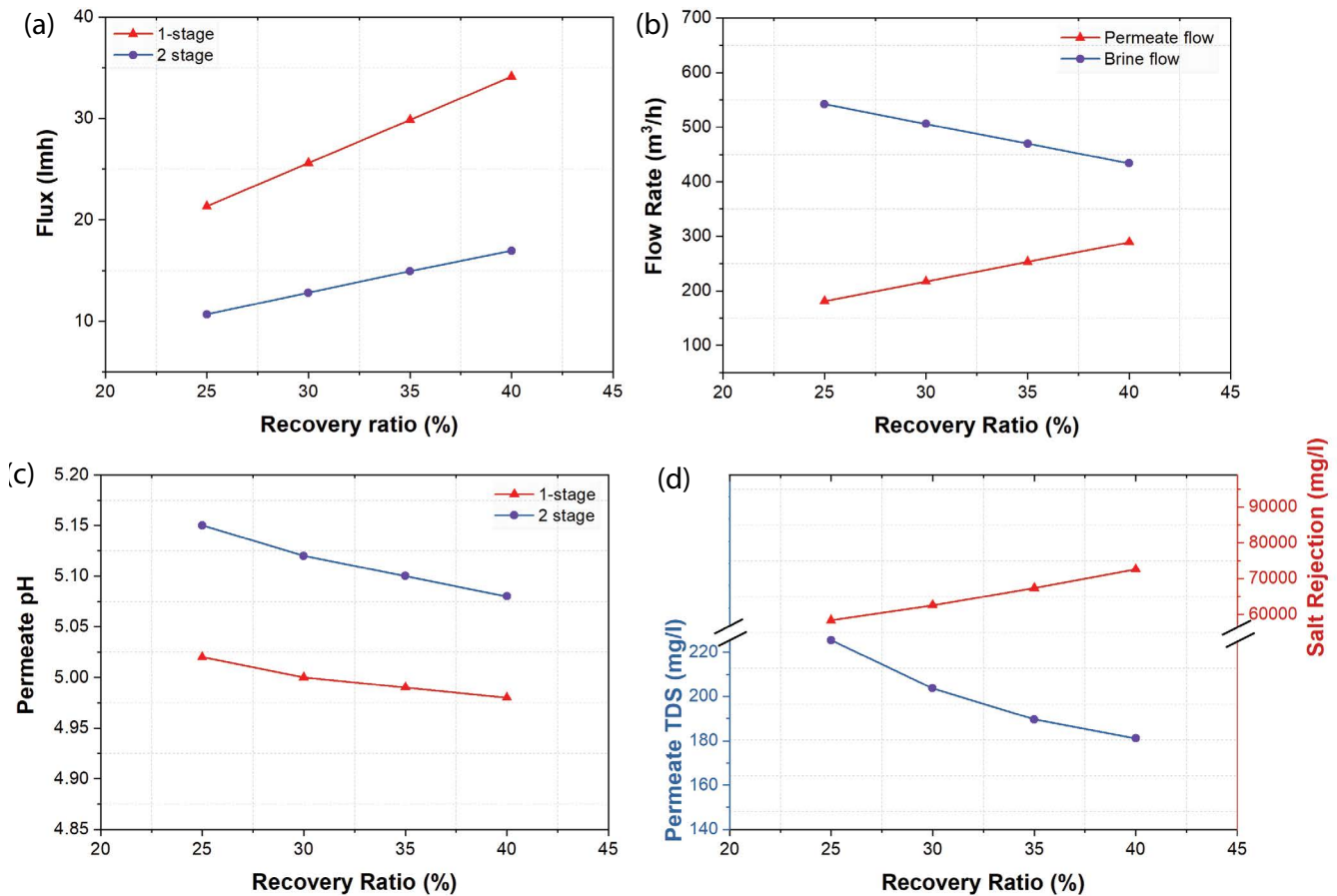
Fig. 12. Effect of recovery ratio on (a) flux, (b) flow rate, (c) permeate pH, (d) salt rejection, and permeate TDS.

matter, minerals, insoluble organic contaminants, and colloidal particles. The TDS gradually increases as the membrane continues to be used over its lifetime.

Fig. 14 indicates that the flow rate of the permeate is almost constant throughout the month of April, except for a few days. The figure also shows that the increase in permeate flow reduces the TDS. If the permeate flow is reduced over the entire period, then fouling of the RO system may occur, and the system would require cleaning. It is, therefore, often worthwhile to apply intense cleaning as it can prolong the life of a membrane. Figs. S1–S11 provide the long-term performance data in terms of permeate flow rate and TDS quality.

7. Economical assessment of the Al-Jubail SWRO plant

An economic analysis of the SWRO system is performed in this section. The cost per unit of energy is the ratio of the total expenses of the power plant to the amount of electricity produced by the power plant over a year. It is important to understand the costs that are incurred over time when carrying out cost analysis; the major economic variables are the costs of development (fixed and variable), the operational and maintenance costs, the economic lifespan, capacity factor, assets, and the discount rates.
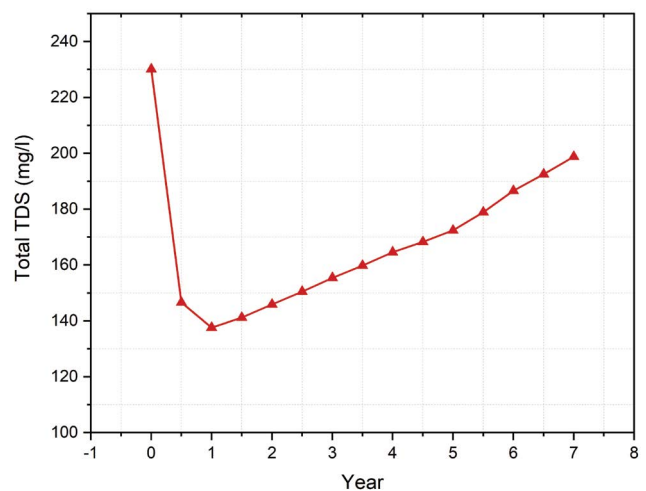

Fig. 13. Effect of membrane life on the total TDS.

CAPEX (capital cost) and OPEX (operating cost) are the main pillars for cost assessment of desalination plants. CAPEX covers many parameters including land, installation charges, equipment's cost, etc.; while, OPEX includes
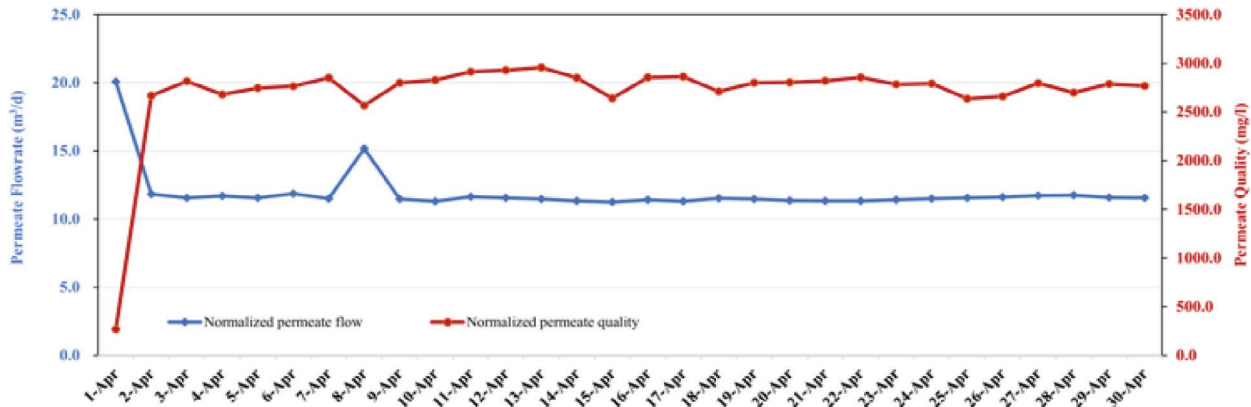
Fig. 14. Permeate flow rate and TDS quality for the month of April.

all the expenses incurred after the commissioning of the plant, which includes replacement of membranes, maintenance cost, brine disposal, energy, labor cost, etc. The annual capital cost can be calculated by multiplying total capital cost and capital recovery factor, which is estimated by using the net present values method defined by the discount rate and future expenses for the specific duration. The expressions for annual recovery factor are given as follows:

$$\left(\text{Recovery factor}\right)_{\text{annual}} = \left[\frac{x\left(1+x\right)^n}{\left(1+x\right)^n - 1}\right] \tag{33}$$

where x is the discount rate and n is the number of future payment. For the amount of water produced, the net annual capital cost can be determined as follows:

$$\left(\text{Capital cost}\right)_{\text{net}} = \frac{\left(\text{Recovery factor}\right) \times \left(\text{capital cost}\right)}{\text{Total capacity of plant}} \tag{34}$$

Based on above expression and by computational assessment, some of the economic parameters of the plant under investigation are listed in Table 6. These parameters were calculated from the well-known desalination and economic program (DEEP) developed by International Atomic Energy Agency. The program works on the Microsoft Excel spreadsheets and is useful for evaluating desalination strategies by calculating estimates of technical performance and costs for various energy and desalination technology configurations. Desalination technology options modeled, include multi-stage flashing (MSF), multi-effect distillation (MED), reverse osmosis (RO) and hybrid options (RO-MSF, RO-MED) while energy source options include nuclear, fossil, renewables and grid electricity (stand-alone RO) [41].

The key parameters affecting the cost of water production are the cost of the plant itself, the aspects of the energy system that are required to meet the energy requirements of the RO system, the properties of the reverse osmosis system, and the economical parameters [50]. The cost of membrane for RO plant can be estimated based on the principle flux and membrane cost with replacement cost

Table 6
Economic parameters of seawater reverse osmosis system

Parameters	Value
Capital recovery factor	0.06
Fuel levelization factor	1.63
Reference net output	20.0 MW
Sp. overnight construction cost	2,530 $
Overnight construction cost	51 M$
Interest during construction	4 M$
Total plant investment	54 M$
Annualized capital cost	3 M$
Annual electricity productivity	121 GWh
Annual fuel cost	24 M$
Total annual cost	28 M$
Levelized power cost	0.229 $/kWh
Sp. levelized power cost	0.027 $/kWh
Sp. fuel cost	0.198 $/kWh
SP. O&M cost	0.003 $/kWh

per year. The addition of this cost in the operating cost of the plant can be calculated by the following expression:

$$\left(\text{Cost of membrane}\right) = \frac{\left(\text{price of membrane}\right) \times \left(\text{replacement rate}\right) \times 1,000}{\text{Membrane flux} \times 8,760} \tag{35}$$

The cost of the RO process relies on the capacity of a system. The levelized cost of electricity is one of the most significant factors in estimating the economic performance of power plants. The relation for the levelized cost of water including the discount rate was calculated by the following set of equations verified by the computational approach, that is,

$$\left(\text{Water cost}\right)_{\text{Levelized}} = \frac{\text{Total cost of life cyle of plant}}{\text{Total production of water}} \tag{36}$$

$$\left(\text{Water cost}\right)_{\text{Discount}} = \frac{\sum_{i=0}^{n}\left(\text{capital cost}\right)_{i}}{\sum_{i=0}^{n}\left(\text{water cost}\right)_{i}} \times \left(1+x\right)_{i} \qquad (37)$$

$$\left(\text{Water cost}\right)_{\text{Annual}} = \frac{\dfrac{\sum_{i=0}^{n}\left(\text{capital cost}\right)_{i}}{\sum_{i=0}^{n}\left(\text{water cost}\right)_{i}} \times \left(1+x\right)_{i}}{\sum_{i=0}^{n}\left(\text{water production cost}\right)_{i}} \qquad (38)$$

The total cost of the water can thus be calculated by using the following relation:

$$\left[W_{P}\right]_{T} = \sum_{i=1}^{n} \frac{\left[\dfrac{\left(X_{c}\right)_{i}}{\left(X_{0}\right)_{i}} \times \dfrac{\left(X_{A}\right)_{i}}{\left(X_{c}\right)_{i}}\right]}{\left(W_{P}\right)_{i}} \qquad (39)$$

where X = cost, O = operation, A = amortization, and W_{P} = water production.

The total costs of the RO process include the intake cost, and pre-treatment or post-treatment systems, among others. The performance and cost parameters are given in Table 7. Two major groups of fixed costs are investment and O&M. O&M costs include the cost of proper operation and maintenance, replacement parts, membrane substitution, and auxiliary consumption expenses. All external consumption, involving chemical dosage, regulation and control, membrane cleaning, blowdown pumping, lighting, and other minor consumables comprise auxiliary consumption.

Several of the economical parameters of the SWRO plant were analyzed in terms of the percentile ratio as shown in Fig. 15, including the material used for construction, the units of electricity used, man power, the required power, and the annual capital cost. It is apparent that the fuel ratio corresponds to the power utilization factor, constituting approximately 62% of the total cost of the plant. This observation was also confirmed by both experimental and computational analysis.

8. Conclusion

This study is a theoretical, experimental, and computational assessment of the Al-Jubail SWRO plant, examining the technical properties and economics of the plant. Actual operational data were used to validate the developed model. It was observed that at a recovery ratio of

Table 7
Desalination economic parameters of seawater reverse osmosis system

| Parameters	Value
Lifetime of water plant	20 y
Water plant operating availability	0.9%
WP planned outage rate	0.032%
WP unplanned outage rate	0.06%
Base unit cost	1,100 \$/(m³/d)
Specific O&M spare parts cost	0.04 \$/m³
Specific O&M chemicals cost for pre-treatment	0.05 \$/m³
Specific O&M chemicals cost for post-treatment	0.02 \$/m³
O&M membrane replacement cost	0.09 \$/m³
Unit size correction factor	1
In/outfall sp. cost factor	7%
Water plant owners cost factor	5%
Water plant cost contingency factor	10%
Water plant O&M insurance cost	1%
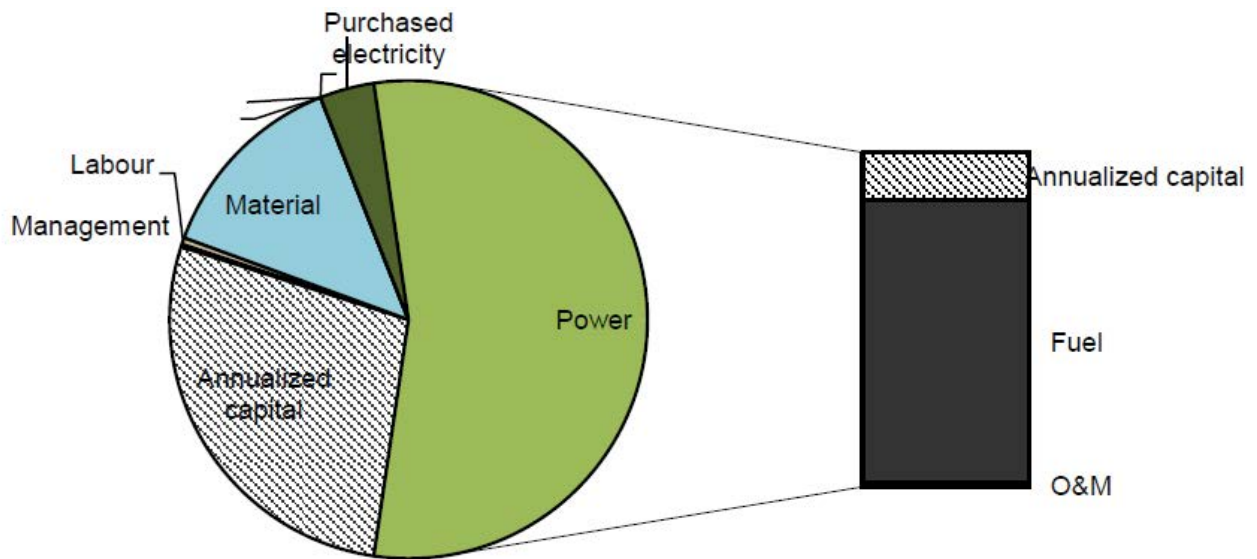
Fig. 15. Capital cost and power distribution of seawater reverse osmosis plant.

75%, the concentrated volume is 25% of the influent volume, indicating that the influent water has an actual concentration of 50%. This ratio was confirmed using the software HOLLOSEP. Some deviations are observed in several parameters (pH: 3.96%, TDS: 0.32%, hardness: 50.10%) describing the plants, as concluded by both the actual plant data and the theoretical-computational model. A maximum flux value of 34.13 lmh was achieved at the highest recovery ratio (40%). In addition, the effect of membrane life on the TDS values was calculated on an annual basis, and it was concluded that the most stable values were achieved during April. The developed model can be used to predict the performance of any plant (using RO). An economic analysis was also performed in order to assess the most cost-effective mode of the plant. The fuel to power ratio was calculated at 28/62, which was validated using actual plant data. This research is useful for confirming and validating various operational RO plants. The development of an optimal design using this model for the safe operation of this type of plant is also suggested.

Acknowledgments

References

[1] P. Asiedu-Boateng, S. Yamoah, F. Ameyaw, S. Dzide, K. Tuffour-Acheampong, Performance analysis of thermal vapour compression desalination system coupled to cogeneration nuclear power plant, Res. J. Appl. Sci. Eng. Technol., 4 (2012) 941–948.

[2] S. Daneshmand, A. Mortaji, Z. Mortaji, Investigation and design seawater desalination with solar energy, Life Sci. J., 9 (2012) 770–773.

[3] G. Fiorenza, V. Sharma, G. Braccio, Techno-economic evaluation of a solar powered water desalination plant, Energy Convers. Manage., 44 (2003) 2217–2240.

[4] I.S. Al-Mutaz, I. Wazeer, Economic optimization of the number of effects for the multieffect desalination plant, Desal. Water Treat., 56 (2015) 2269–2275.

[5] T. Mezher, H. Fath, Z. Abbas, A. Khaled, Techno-economic assessment and environmental impacts of desalination technologies, Desalination, 266 (2011) 263–273.

[6] A. Alsairafi, I. Al-Shehaima, M. Darwish, Efficiency improvement and exergy destruction reduction by combining a power and a multi-effect boiling desalination plant, J. Eng. Res., 1 (2013) 289–315.

[7] I.-S. Park, S.-M. Park, J.-S. Ha, Design and application of thermal vapor compressor for multi-effect desalination plant, Desalination, 182 (2005) 199–208.

[8] H.M. Ettouney, H. El-Dessouky, A simulator for thermal desalination processes, Desalination, 125 (1999) 277–291.

[9] P.A. Claisse, Transport Properties of Concrete: Measurements and Applications, Woodhead Publishing, Cambridge, 2014, pp. 1–16.

[10] K.P. Lee, T.C. Arnot, D. Mattia, A review of reverse osmosis membrane materials for desalination—development to date and future potential, J. Membr. Sci., 370 (2011) 1–22.

[11] N.M. Al-Bastaki, A. Abbas, Modeling an industrial reverse osmosis unit, Desalination, 126 (1999) 33–39.

[12] T. Kaghazchi, M. Mehri, M.T. Ravanchi, A. Kargari, A mathematical modeling of two industrial seawater desalination plants in the Persian Gulf region, Desalination, 252 (2010) 135–142.

[13] M.S. Atab, A. Smallbone, A. Roskilly, An operational and economic study of a reverse osmosis desalination system for potable water and land irrigation, Desalination, 397 (2016) 174–184.

[14] M. Al-Sahali, S. Al-Qattan, Performance analysis of small capacity reverse osmosis desalination plants, Kuwait J. Sci. Eng., 39 (2012) 231–253.

[15] K.A. Al-Shayji, Y. Liu, Predictive modeling of large-scale commercial water desalination plants: data-based neural network and model-based process simulation, Ind. Eng. Chem. Res., 41 (2002) 6460–6474.

[16] A.M. Hassan, A. Abanmy, M. Al-Thobiety, T. Mani, T. Al-Luhibi, I. Al-Masudi, A.A. Al-Gherier, L. Bakheet, M.M. Amri, K. Atiya, Performance Evaluation of SWCC SWRO Plants Part II, in: Proceedings of IDA World Conference, International Desalination Association, Topsfield, MA, Washington, D.C., 1991, pp. 412–439.

[17] O. Hamed, A. Moet, T. Abdelrahman, A. Zamamiri, Performance Analysis of Sea Water Reverse Osmosis Plants, in: IDA World Congress on "Desalination and Water Science" Abu Dhabi, 1995, pp. 13–23.

[18] A.S. Al-Mobayed, F.M. Mubeen, S. Balaji, Comparison of the performance of hollow fine fiber and spiral-wound membranes in the Al-Jubail SWRO desalination plant, Desalination, 178 (2005) 273–286.

[19] I.S. Al-Mutaz, B.A. Al-Sultan, Prediction performance of RO desalination plants, Desalination, 120 (1998) 153–160.

[20] A. Jiang, Q. Ding, J. Wang, S. Jiangzhou, W. Cheng, C. Xing, Mathematical modeling and simulation of SWRO process based on simultaneous method, J. Appl. Math., 2014 (2014) 1–11.

[21] M. Goosen, S. Sablani, M.D. Cin, M. Wilf, Effect of cyclic changes in temperature and pressure on permeation properties of composite polyamide seawater reverse osmosis membranes, Sep. Sci. Technol., 46 (2010) 14–26.

[22] D. Ghernaout, Reverse osmosis process membranes modeling–a historical overview, J. Civil Construct. Environ. Eng. Civil, 2 (2017) 112–122.

[23] T. Qiu, P. Davies, Concentration polarization model of spiral-wound membrane modules with application to batch-mode RO desalination of brackish water, Desalination, 368 (2015) 36–47.

[24] D.Y. Kim, M.H. Lee, B. Gu, J.H. Kim, S. Lee, D.R. Yang, Modeling of solute transport in multi-component solution for reverse osmosis membranes, Desal. Water Treat., 15 (2010) 20–28.

[25] M. Khanarmuei, H. Ahmadisedigh, I. Ebrahimi, L. Gosselin, H. Mokhtari, Comparative design of plug and recirculation RO systems; thermoeconomic: case study, Energy, 121 (2017) 205–219.

[26] J.G. Wijmans, R.W. Baker, The solution-diffusion model: a review, J. Membr. Sci., 107 (1995) 1–21.

[27] S. Lee, R.M. Lueptow, Membrane rejection of nitrogen compounds, Environ. Sci. Technol., 35 (2001) 3008–3018.

[28] R. Rautenbach, F. Helmus, Some considerations on mass-transfer resistances in solution—diffusion-type membrane processes, J. Membr. Sci., 87 (1994) 171–180.

[29] R.V. Linares, Z. Li, S. Sarp, S.S. Bucs, G. Amy, J.S. Vrouwenvelder, Forward osmosis niches in seawater desalination and wastewater reuse, Water Res., 66 (2014) 122–139.

[30] G. Schock, A. Miquel, Mass transfer and pressure loss in spiral wound modules, Desalination, 64 (1987) 339–352.

[31] M. Sekino, Performance data analysis for hollow-fiber reverse-osmosis modules in seawater desalination plants, Kagaku kōgaku ronbunshū, 20 (1994) 574–579.

[32] M. Taniguchi, S. Kimura, Estimation of transport parameters of RO membranes for seawater desalination, AIChE J., 46 (2000) 1967–1973.

[33] M. Taniguchi, M. Kurihara, S. Kimura, Behavior of a reverse osmosis plant adopting a brine conversion two-stage process and its computer simulation, J. Membr. Sci., 183 (2001) 249–257.

[34] C. Chen, H. Qin, A mathematical modeling of the reverse osmosis concentration process of a glucose solution, Processes, 7 (2019) 271.

[35] J.A. Howell, V. Sanchez, R.W. Field, Membranes in Bioprocessing: Theory and Applications, Springer Netherlands, 2012, pp. 55–112.

[36] H.T. El-Dessouky, H.M. Ettouney, Fundamentals of Salt Water Desalination, Elsevier Science, New York, 2002, pp. 409–437.

[37] G. Amy, N. Ghaffour, Z. Li, L. Francis, R.V. Linares, T. Missimer, S. Lattemann, Membrane-based seawater desalination: present and future prospects, Desalination, 401 (2017) 16–21.

[38] J. Kim, K. Park, D.R. Yang, S. Hong, A comprehensive review of energy consumption of seawater reverse osmosis desalination plants, Appl. Energy, 254 (2019) 113652.

[39] J. Kim, K. Park, S. Hong, Optimization of two-stage seawater reverse osmosis membrane processes with practical design aspects for improving energy efficiency, J. Membr. Sci., 601 (2020) 117889.

[40] A.H. Gulamhusein, A.S. Al Sheikh Khalil, I.A. Fatah, R. Boda, S. Rybar, IMS SWRO Kindasa—Two years of operational experience, Desal. Water Treat., 10 (2009) 245–254.

[41] R. de Morales, Planta desaladora de agua de mar con capacidad para producir 60.000 m³/día de agua apta para riego, Infoenviro, (2016) 35–50.

[42] S. Meyer-Steele, A. von Gottberg, J.L. Talavera, seawater reverse osmosis plants in the Caribbean recover energy and brine and reduce costs, (2005).

[43] R. Lemes, R. Falcon, R. Arocha, J. Curbelo, V. Platas, L.D. Lorenzo, Different designs in energy savings of

[44] T. Hamano, Operation of Fukuoka sea water desalination plant, Bull. Soc. Sea Water Sci. Jpn., 60 (2006) 415–421.

[45] F. Rezazadeh, W.F. Gale, M. Akram, K.J. Hughes, M. Pourkashanian, Performance evaluation and optimisation of post combustion CO_2 capture processes for natural gas applications at pilot scale via a verified rate-based model, Int. J. Greenhouse Gas Control, 53 (2016) 243–253.

[46] F. Mahmoudi, A. Akbarzadeh, Sustainable Desalination by Permeate Gap Membrane Distillation Technology, in: Emerging Technologies for Sustainable Desalination Handbook, Elsevier, Oxford, 2018, pp. 157–204.

[47] A. Schäfer, A. Broeckmann, B. Richards, Membranes and renewable energy—a new era of sustainable development for developing countries, Membr. Technol., 2005 (2005) 6–10.

[48] S. Sourirajan, The science of reverse osmosis-mechanisms, membranes, transport and applications, Pure Appl. Chem., 50 (1978) 593–615.

[49] S. Sourirajan, The Science of Reverse Osmosis-Mechanisms, Membranes, Transport and Applications, in: Chemistry for the Welfare of Mankind, Elsevier, Great Britain, 1979, pp. 593–615.

[50] Z. Triki, M. Bouaziz, M. Boumaza, Techno-economic feasibility of wind-powered reverse osmosis brackish water desalination systems in southern Algeria, Desal. Water Treat., 52 (2014) 1745–1760.

SWRO Plant of Las Palmas III, Desal. Water Treat., 51 (2013) 749–758.
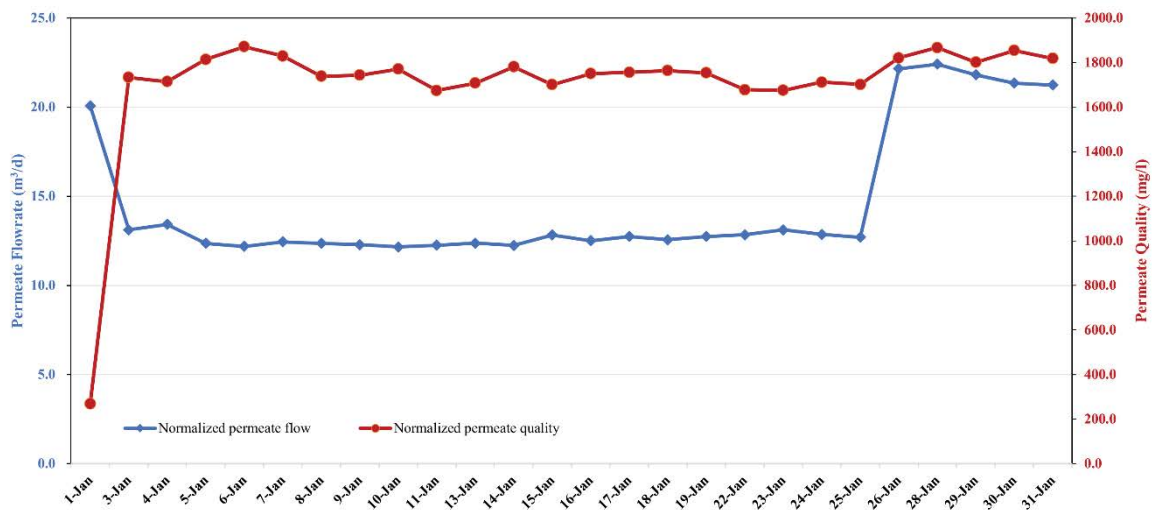
Supporting information

Fig. S1. Permeate flow rate and TDS quality for the month of January.
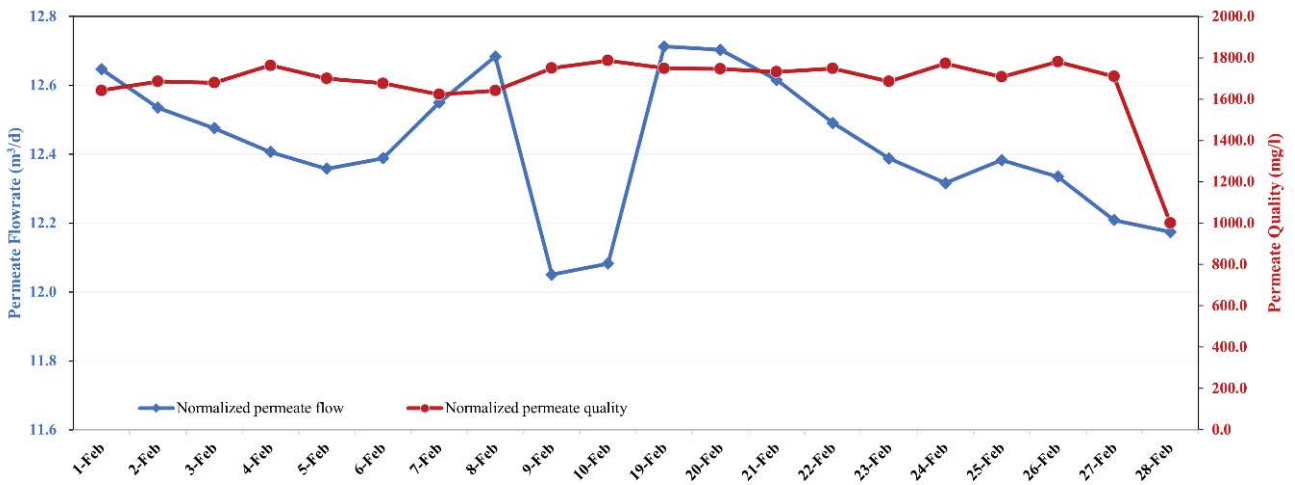
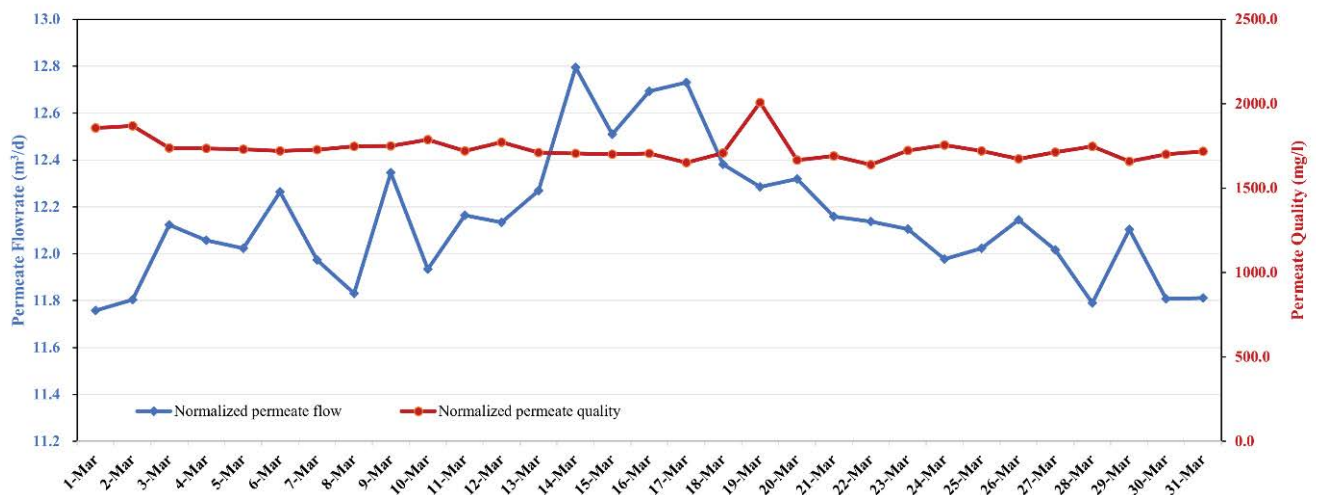Fig. S2. Permeate flow rate and TDS quality for the month of February.

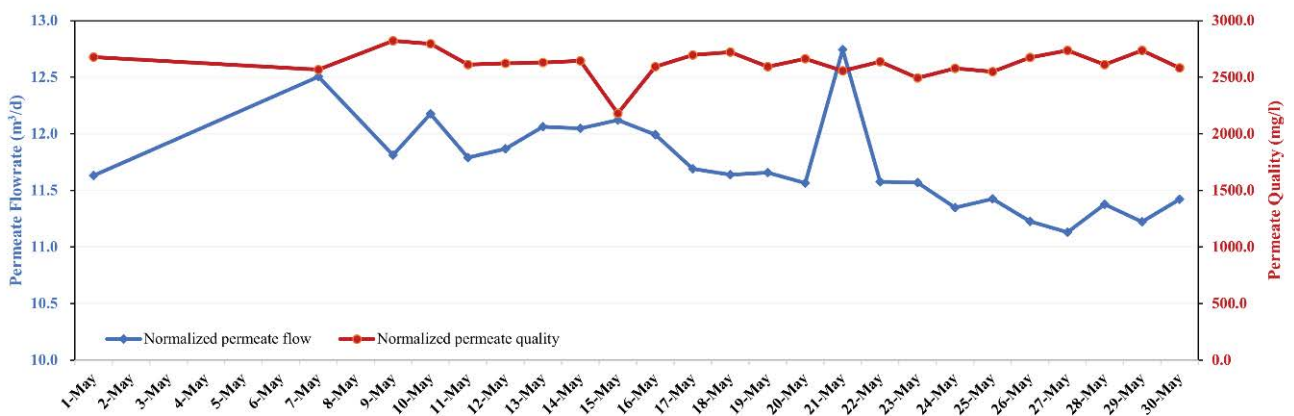Fig. S3. Permeate flow rate and TDS quality for the month of March.

Fig. S4. Permeate flow rate and TDS quality for the month of May.
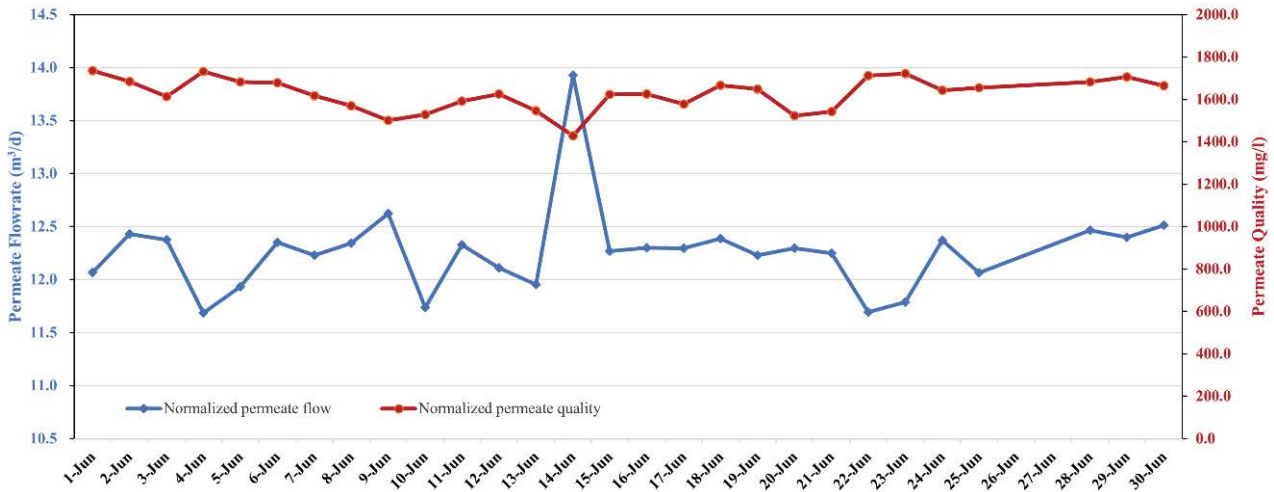
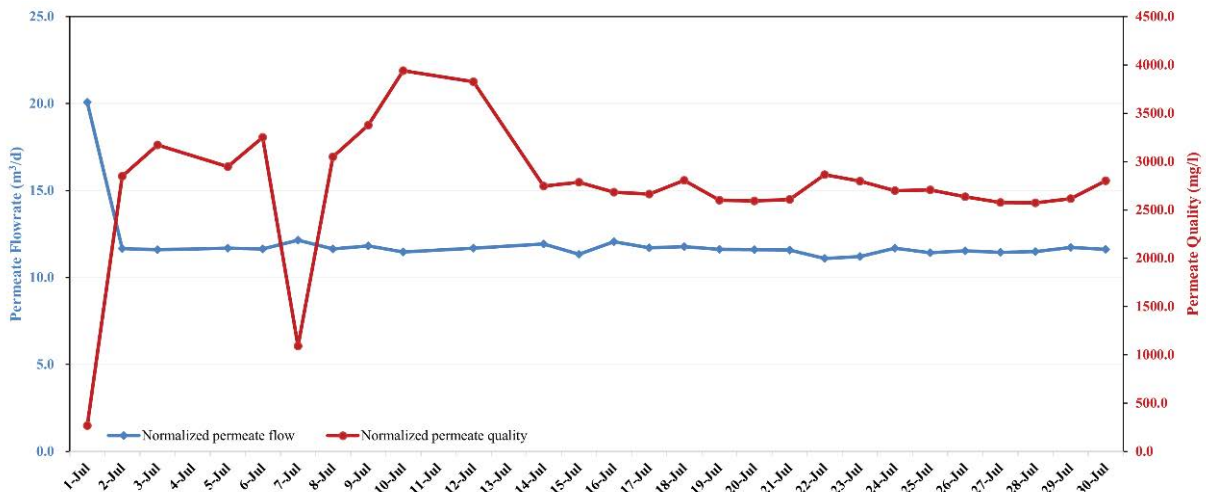Fig. S5. Permeate flow rate and TDS quality for the month of June.

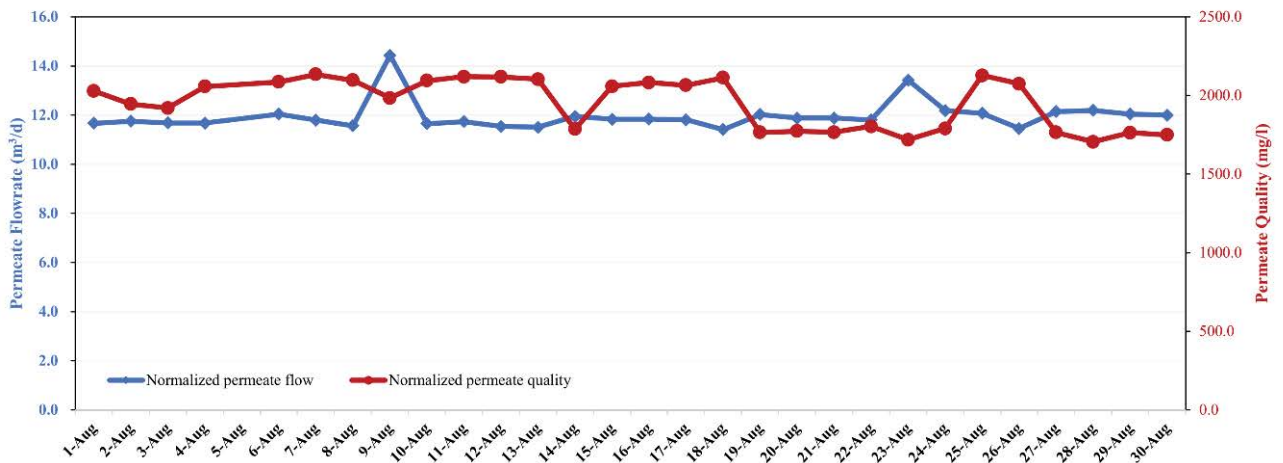Fig. S6. Permeate flow rate and TDS quality for the month of July.

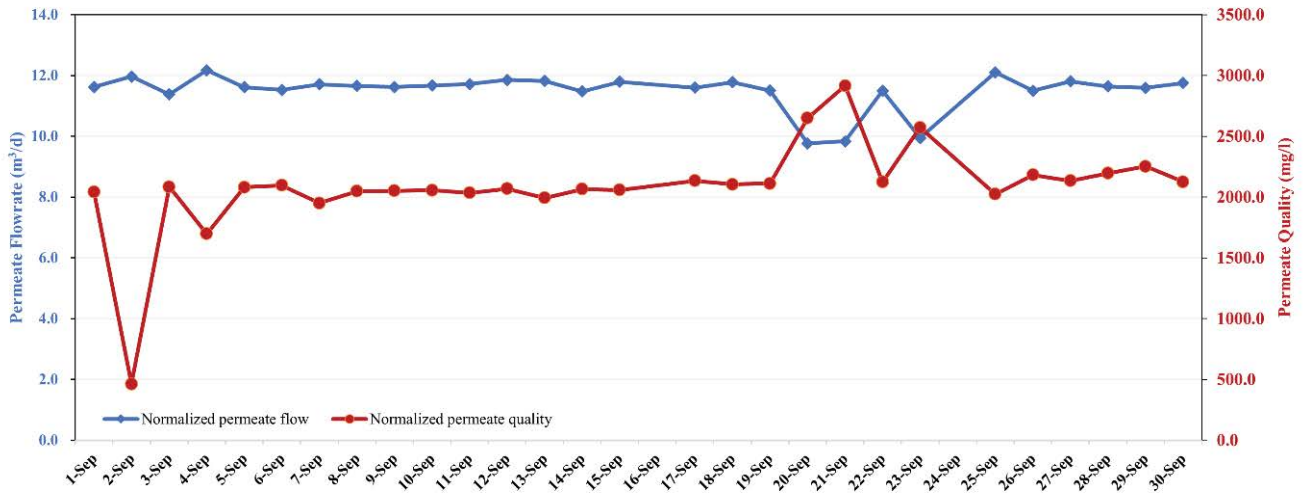Fig. S7. Permeate flow rate and TDS quality for the month of August.

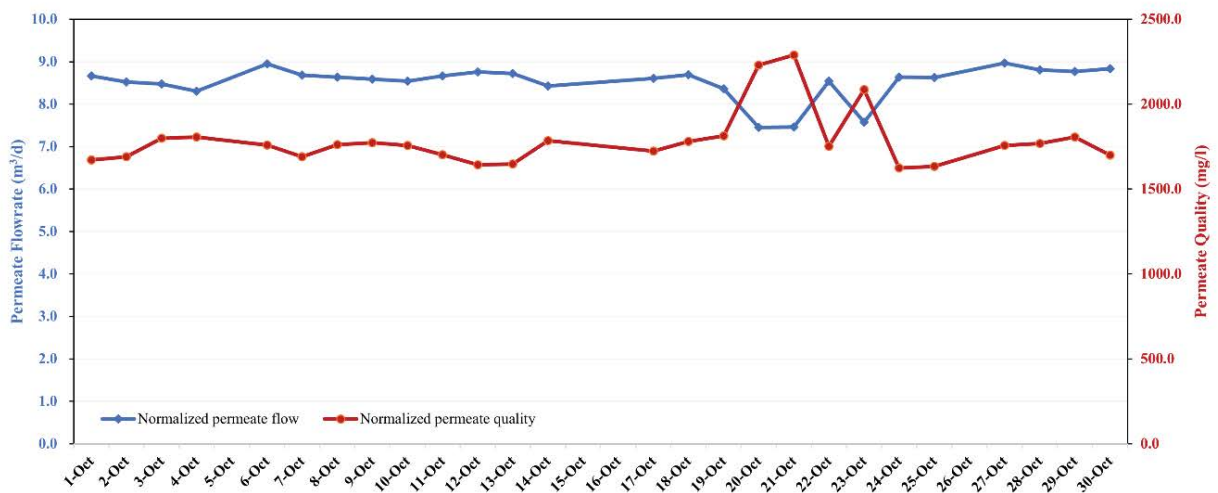Fig. S8. Permeate flow rate and TDS quality for the month of September.

Fig. S9. Permeate flow rate and TDS quality for the month of October.
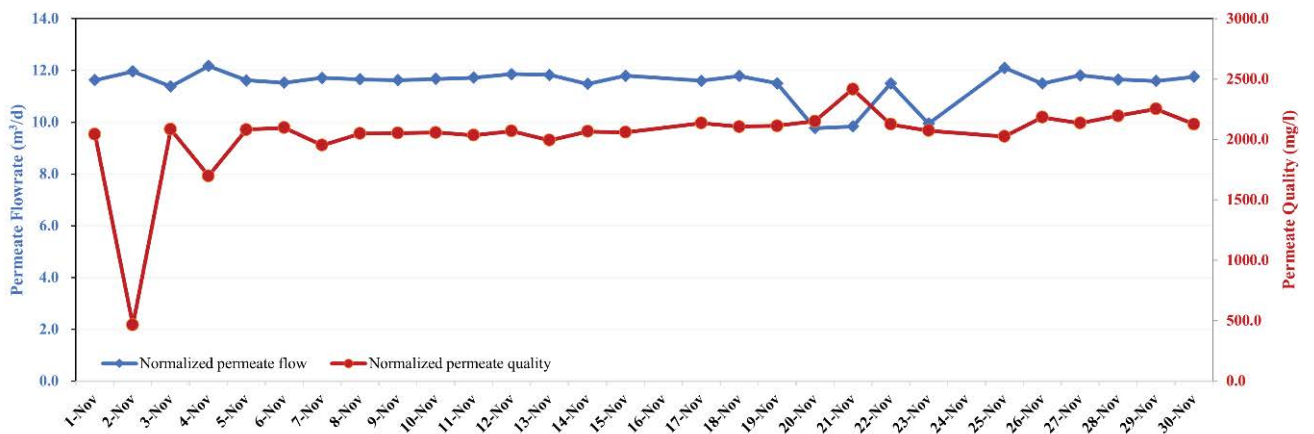

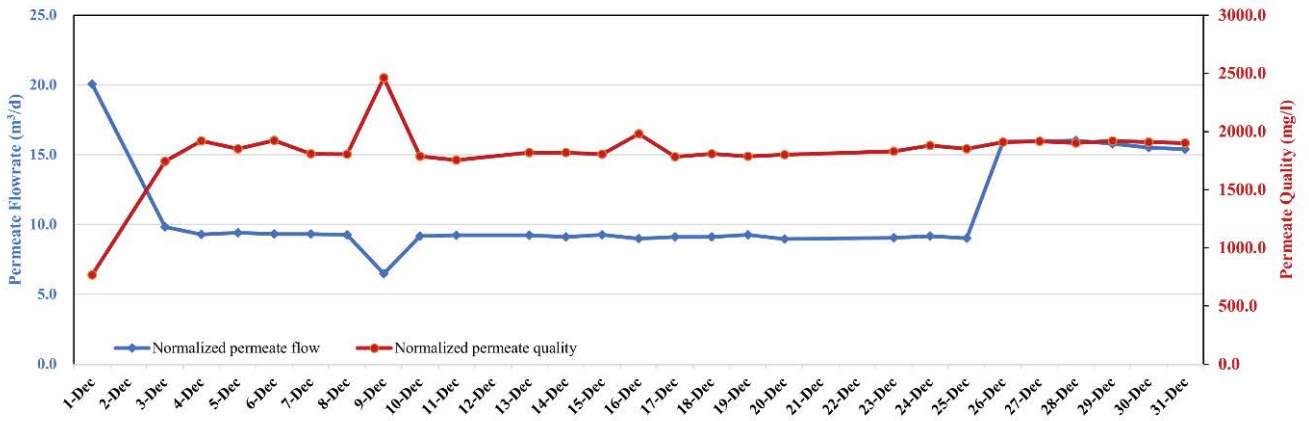Fig. S10. Permeate flow rate and TDS quality for the month of November.

Fig. S11. Permeate flow rate and TDS quality for the month of December.